

**Conflicts of interest and sources of funding:** The authors state that there are no conflicts of interest to disclose.

**Ashwin S. Akki, Danielle K. Harrell, Kaitlin D. Weaver, Ashwini K. Esnakula, Archana Shenoy**

*University of Florida, Department of Pathology, Immunology and Laboratory Medicine, Gainesville, FL, USA*

Contact Dr Ashwin S. Akki.

E-mail: [a.akkii@ufl.edu](mailto:a.akkii@ufl.edu)

1. Skapek SX, Ferrari A, Gupta AA, *et al.* Rhabdomyosarcoma. *Nat Rev Dis Prim* 2019; 5: 1–19.
2. Nascimento AF, Barr FG. Spindle cell/sclerosing rhabdomyosarcoma. In: Fletcher CDM, Bridge JA, Hogendoorn PCW, *et al.*, editors. *WHO Classification of Tumors of Soft Tissue and Bone*. 4th ed. Lyon: IARC Press, 2013; 134–5.
3. Parham DM, Barr FG, Montgomery ENA. Skeletal muscle tumors. In: Fletcher CDM, Bridge JA, Hogendoorn PCW, *et al.*, editors. *WHO Classification of Tumors of Soft Tissue and Bone*. 4th ed. Lyon: IARC Press, 2013; 123–35.
4. Cavazzana AO, Schmidt D, Ninfo V, *et al.* Spindle cell rhabdomyosarcoma. A prognostically favorable variant of rhabdomyosarcoma. *Am J Surg Pathol* 1992; 16: 229–35.
5. Mentzel T, Katenkamp D. Sclerosing, pseudovascular rhabdomyosarcoma in adults. Clinicopathological and immunohistochemical analysis of three cases. *Virchows Arch* 2000; 436: 305–11.
6. Agaram NP, LaQuaglia MP, Alaggio R, *et al.* MYOD1-mutant spindle cell and sclerosing rhabdomyosarcoma: an aggressive subtype irrespective of age. A reappraisal for molecular classification and risk stratification. *Mod Pathol* 2019; 32: 27–36.
7. Zhao Z, Yin Y, Zhang J, *et al.* Spindle cell/sclerosing rhabdomyosarcoma: case series from a single institution emphasizing morphology, immunohistochemistry and follow-up. *Int J Clin Exp Pathol* 2015; 8: 13814–20.
8. Folpe AL, McKenney JK, Bridge JA, *et al.* Sclerosing rhabdomyosarcoma in adults: report of four cases of a hyalinizing, matrix-rich variant of rhabdomyosarcoma that may be confused with osteosarcoma, chondrosarcoma, or angiosarcoma. *Am J Surg Pathol* 2002; 26: 1175–83.
9. Hornick JL, Nielsen GP. Beyond “Triton” malignant peripheral nerve sheath tumors with complete heterologous rhabdomyoblastic differentiation mimicking spindle cell rhabdomyosarcoma. *Am J Surg Pathol* 2019; 43: 1323–30.
10. Rekhi B, Upadhyay P, Ramteke MP, *et al.* MYOD1 (L122R) mutations are associated with spindle cell and sclerosing rhabdomyosarcomas with aggressive clinical outcomes. *Mod Pathol* 2016; 29: 1532–40.
11. Alaggio R, Zhang L, Sung Y-S, *et al.* A molecular study of pediatric spindle and sclerosing rhabdomyosarcoma. *Am J Surg Pathol* 2016; 40: 224–35.
12. Watson S, Perrin V, Guillemot D, *et al.* Transcriptomic definition of molecular subgroups of small round cell sarcomas. *J Pathol* 2018; 245: 29–40.

DOI: <https://doi.org/10.1016/j.pathol.2019.07.010>

## Intra-abdominal pulmonary sequestration: a rare diagnostic pitfall on EUS-FNA



Sir,

Pulmonary sequestration (PS) is a rare congenital malformation characterised by a segment of pulmonary tissue that does not communicate with the tracheobronchial tree, and that draws its blood supply directly from the systemic arterial tree. PS is most frequently diagnosed antenatally and during childhood, with imaging classically showing a variably cystic lesion with a systemic feeding vessel. Intralobar sequestration

(ILS), being the more common type, is localised within the normal pulmonary parenchyma. Extralobar sequestration (ELS) is relatively uncommon, and features lung tissue that is found external to the visceral pleura.<sup>1</sup> ELS can occur in the thorax (90%), mediastinum, pericardium, and within or below the diaphragm.<sup>2</sup> Thus, ELS poses a significant diagnostic challenge, particularly in adults.

We document an unusual case of intra-abdominal ELS in an adult, presenting the findings on endoscopic ultrasound (EUS)-guided fine needle aspiration (FNA), together with a literature review of this rare entity.

A 67-year-old Chinese female was incidentally found on computed tomography (CT) scan to have a well-defined, low-density retroperitoneal mass measuring 4.9 × 2.0 × 2.9 cm with small mildly enhancing areas and a speck of calcification. It was medial to the spleen and above the left adrenal gland. The possibility of a retroperitoneal haemangioma or lymphangioma was raised.

EUS revealed a 3.5 × 2.7 cm solid-cystic lesion adjacent to the pancreatic tail and spleen. Transgastric EUS-guided FNA was performed. The smears were hypocellular, showing scattered clusters of bland columnar epithelial cells, some with discernible terminal bars and cilia (Fig. 1), on a background of mucoid material. Occasional macrophages were also present. No significant nuclear atypia, necrosis or mitotic activity were seen. The cytological diagnosis was ‘cyst contents; mucinous cystic neoplasm not fully excluded’.

Laparoscopic excision was performed, and an encapsulated, retroperitoneal parasplenic, partially cystic mass measuring approximately 4 × 3 × 2 cm was removed. The specimen comprised three friable fragments of spongy red to tan coloured tissue admixed with mucinous material, altogether measuring 6 × 3 × 2 cm. Microscopy revealed a solid-cystic lesion with a thin fibrous rim composed of variably sized, mucin-filled cystic spaces lined by ciliated respiratory type epithelium with occasional goblet cells (Fig. 2). An island of cartilage was noted adjacent to a cystic space, reminiscent of a bronchial structure. Serous and mucous peribronchial-like glands were also identified. The intervening stroma was composed of bundles of smooth muscle and muscular arteries. Patchy chronic inflammation was present. Other areas showed partially collapsed alveolar spaces with scattered intra-alveolar macrophages. No significant nuclear atypia, mitotic activity or necrosis were identified. The morphological features were compatible with those of pulmonary sequestration.

Post-operative recovery was uneventful. Follow-up CT scan revealed a residual lesion measuring 3.2 × 1.5 cm, which remained stable over the next 2 years.

Intra-abdominal pulmonary sequestration (IAPS) is extremely uncommon, comprising 10–15% of ELS cases and 2–5% of cases of PS.<sup>3</sup> In adults, IAPS is usually discovered incidentally at autopsy or during other surgical or radiological procedures.<sup>1</sup> ELS is believed to arise from an outpouching of the foregut that is structurally separate from the normally developing lung, with a systemic arterial supply draining into the azygos system.<sup>1</sup> It is usually single but can sometimes occur as multiple lesions. Association with the gastrointestinal tract occurs frequently at the region of the lower oesophagus and stomach. ELS may be associated with other congenital abnormalities such as diaphragmatic hernia. Superimposed infection is rare, as ELS is anatomically

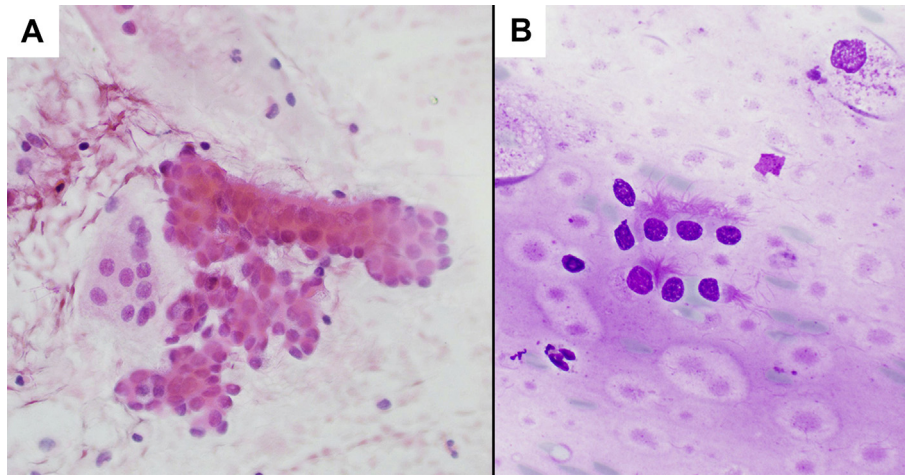


**Fig. 1** Cytological findings of the trans-gastric EUS-FNA. (A,B) High power microscopy showing bland ciliated columnar cells on a background of thin mucoid material (A, alcohol-fixed Papanicolaou-stained smear; B, air-dried Hemacolor-stained smear).

separate from the tracheobronchial tree, with its own pleural investment.<sup>4</sup> Rare cases of malignancy have been documented, including an adenocarcinoma.<sup>5</sup> Table 1 summarises the current literature of histologically-confirmed cases. Only one of the seven cases had a presumptive pre-operative diagnosis of ELS, which was based on imaging.<sup>6</sup> Four patients underwent percutaneous pre-operative biopsy with ultrasound (US) or CT-guided FNA; two cases also underwent CT-guided core biopsy. The pre-operative diagnoses were mainly descriptive, with one case raising the possibility of a non-representative sample.<sup>7</sup> None of the cases had a pre-operative cytological diagnosis of ELS. To date, this is the first case of an EUS-guided FNA for such a lesion; with a non-percutaneous needle route.

In adults, the differential diagnosis of intra-abdominal cystic lesions is broad and includes cystic pancreatic lesions, foregut and gastric/gastro-enteric duplication cysts, bronchogenic cysts, intra-abdominal lymphangiomas and benign cystic mesothelioma.

In females, large cystic adnexal masses (e.g., cystic teratomas, cystic ovarian epithelial neoplasms) may also be considered. A combination of imaging, relevant laboratory investigations (e.g., tumour markers) and, potentially, cytological samples would usually suggest this. Primary retroperitoneal teratoma may also occur in children, but biopsy contains tissues representing multiple germ layers.<sup>1</sup>

Cystic pancreatic lesions are often evaluated pre-operatively by EUS-guided FNA. The main differential diagnoses include pseudocyst, mucin producing neoplasms [intraductal papillary mucinous neoplasm (IPMN), mucinous cystic neoplasm (MCN)], serous cystadenoma, solid pseudopapillary tumour and tumours with cystic degeneration, e.g., endocrine tumours. The diagnostic workup should include the patient demographics (e.g., MCNs usually occur in females); clinical findings (e.g., pseudocysts are associated with pancreatitis); EUS findings (e.g., IPMNs are connected to the pancreatic ductal system); cytological findings and biochemical and/or molecular cyst

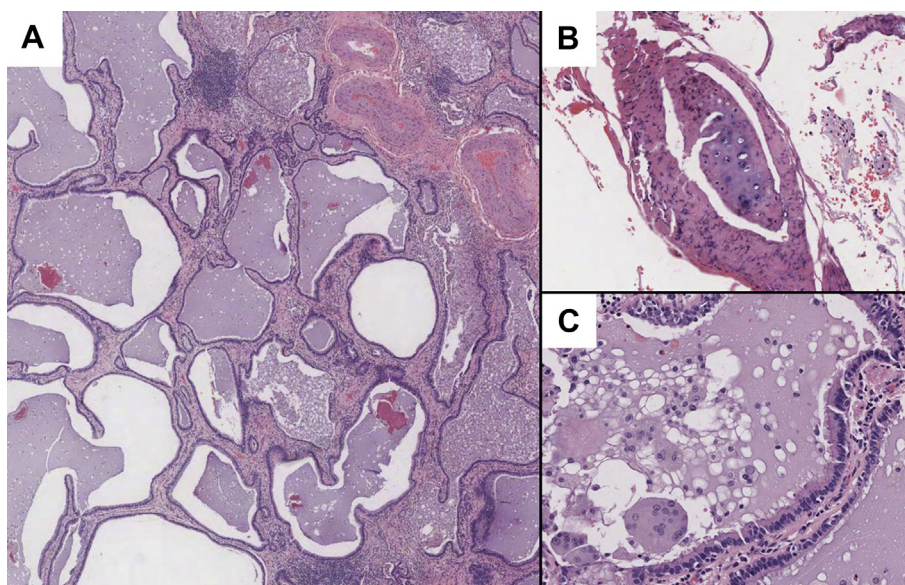


**Fig. 2** Histological findings of the excisional biopsy (H&E). (A) Low power examination showed variably sized cystic spaces containing basophilic mucinous material. (B) An island of cartilage is also noted adjacent to a cystic space, reminiscent of a bronchial structure. (C) Higher magnification showing ciliated columnar cells lining the cystic spaces.

**Table 1** Summary of IAPS cases in the current literature

Case no., demographics, reference	Clinical presentation	Radiological findings	Pre-operative biopsy	Pre-operative diagnosis
1. 64/F Armbruster <i>et al.</i> , 2004 <sup>7</sup>	Incidental finding	US and CT abdomen: well-defined solid-cystic tumour, connected to tail of pancreas	FNA: fatty tissue, fibroblasts and epithelial cells without abnormalities	Pancreatic tail tumour
2. 55/F Rajendiran <i>et al.</i> , 2003 <sup>1</sup>	Incidental finding	CT abdomen: 6.4 cm heterogeneously enhancing mass in left suprarenal space contiguous with left adrenal gland, stomach and spleen; partially adherent to the hemidiaphragm and left adrenal gland	CT guided FNA: skeletal muscle, fibroadipose tissue, macrophages and benign respiratory type ciliated epithelial cells CT guided core biopsy: benign respiratory type epithelial cells	Imaging: bronchogenic cyst favoured; differentials of herniated pulmonary parenchyma or teratoma Cytology: raised possibility of FNA being non-representative
3. 45/F Franko <i>et al.</i> , 2006 <sup>4</sup>	Epigastric pain	CT scan: 4.3 cm heterogenous retroperitoneal mass, beneath diaphragm in region of left adrenal gland; calcification present	CT-guided FNA and core biopsy: ciliated respiratory type epithelium	None
4. 40/M Yang <i>et al.</i> , 2012 <sup>2</sup>	Left flank pain	CT scan: 11.3 cm multiloculated cystic non-enhancing left retroperitoneal mass with a 5.5 cm solid component, in contact with adrenal gland; calcification present	Nil	Retroperitoneal or adrenal tumour
5. 34/M Kim <i>et al.</i> , 2005 <sup>3</sup>	Epigastric discomfort and fever	Chest X-ray (CXR): elevated left hemidiaphragm and calcified mass in left upper abdomen. CT scan: 16 cm multiseptated dumbbell-shaped cystic tumour with calcification in upper anterior aspect of left kidney	Ultrasound guided FNA: 850 mL of pus drained	Subphrenic abscess or pancreatic pseudocyst
6. 40/F Schulz <i>et al.</i> , 2010 <sup>6</sup>	Left sided chest pain and cough	MRI: left lung lower lobe lesion measuring 5.1 cm and a subphrenic complex cystic mass lesion measuring 1.5 cm with aberrant arterial supply	Nil	ILS and subdiaphragmatic lesion consistent with ELS
7. 48/F Lee <i>et al.</i> , 2014 <sup>12</sup>	Intermittent abdominal pain	CT scan: left hemidiaphragmatic rounded mass measuring 4 cm with calcification	Nil	None

CT, computed tomography; ELS, extralobar sequestration; FNA, fine needle aspiration; IAPS, intra-abdominal pulmonary sequestration; ILS, intralobar sequestration; MRI, magnetic resonance imaging.

fluid analysis. Generally, ciliated cells are not a feature of pancreatic cysts.

Gastro-enteric duplication cysts usually occur in children; however, they may present in adulthood with gastrointestinal symptoms and occasionally a palpable abdominal mass.<sup>8</sup> Imaging may suggest the diagnosis. Histologically, they are usually lined by gastrointestinal type epithelium rather than ciliated columnar cells.

Ciliated hepatic foregut cysts are rare benign cysts usually affecting males and commonly located in the medial segment of the left hepatic lobe. They are hypoechoic on US but hyperdense on CT. FNA yields benign ciliated columnar cells in a mucinous background, similar to our findings in this patient. Histology shows a ciliated epithelial lining, loose connective tissue, smooth muscle, and a fibrous capsule.

Intra-abdominal bronchogenic cysts are often retroperitoneal. In a series of five cases, three were close to the pancreatic tail and/or left adrenal gland.<sup>9</sup> Similar to IAPS, radiology may also suggest a lymphangiomatous or pancreatic mucinous lesion, while FNA may contain mucin, adding to the potential pitfall. Histology reveals cystic spaces lined

by ciliated columnar cells, and sometimes peri-bronchial-type glands, but unlike ELS, no lung parenchyma.

Intra-abdominal lymphangiomas are rare benign congenital lesions occurring most commonly in the mesentery, followed by omentum, mesocolon and retroperitoneum.<sup>10</sup> Imaging reveals well-defined multicystic cavities with thin septa. The FNA yields chylous milky-white fluid and smears show numerous lymphocytes in a proteinaceous background. On histology, there are dilated endothelial-lined lymphatic spaces filled with eosinophilic material.<sup>10</sup>

Benign cystic mesothelioma is yet another cystic intra-abdominal neoplasm that may radiologically resemble lymphangioma or a cystic adnexal mass. Cytological aspirates may contain bland mesothelial cells which are helpful in the differential diagnosis.<sup>11</sup>

In the cytological workup of intra-abdominal cystic lesions, the specific finding of ciliated columnar cells raises possibilities such as ciliated foregut cyst, teratoma, intra-abdominal bronchogenic cyst, and IAPS.<sup>1</sup> The cytological findings need to be interpreted in conjunction with clinical features such as gender, age, location and radiological appearance. When a specific diagnosis is not possible, a more

descriptive diagnosis may be given, with a comment on the likely benign nature of these lesions.

Current literature shows that pre-operative diagnosis of ELS is challenging, even with imaging and cytology. The initial working diagnosis prior to surgical resection in our case was that of a parasplenic mucinous cystic lesion. On histology, ELS shows dilated bronchi and bronchioles, alveolar ducts, and alveoli. A well-formed bronchus may be present, but dilated bronchial structures surrounded by a fibromuscular wall with a cartilage plate are more frequently seen. The presence of alveolar structures excludes a bronchogenic cyst.<sup>1</sup> Superimposed infarction, arteritis, infection, and congenital cystic adenomatoid malformations may alter the microscopic features and potentially mimic malignancy (e.g., adenocarcinoma). Herniation of the lung outside the thoracic cavity is unusual and a combination of clinical and radiological findings will be helpful in its exclusion.<sup>1</sup>

The treatment of choice for ELS is surgical excision. It is prudent for pathologists to consider ELS in the differential diagnosis of subdiaphragmatic intra-abdominal lesions in which FNA shows unusual features such as respiratory epithelium or cartilage. Specific imaging investigations may then be applied to ascertain the pre-operative diagnosis of this rare entity, so that appropriate surgical treatment can be planned.

**Conflicts of interest and sources of funding:** The authors state that there are no conflicts of interest to disclose.

**Irfan Sagir Khan<sup>1</sup>, Darren Chua<sup>2</sup>, Benjamin Wong<sup>3</sup>, Shi Wang<sup>1</sup>, Min En Nga<sup>1</sup>**

<sup>1</sup>National University Health System, Singapore; <sup>2</sup>Yong Loo Lin School of Medicine, National University of Singapore, Singapore; <sup>3</sup>Woodlands Health Campus, Singapore

Contact Dr Irfan Sagir Khan.

E-mail: [irfan\\_sagir\\_khan@nuhs.edu.sg](mailto:irfan_sagir_khan@nuhs.edu.sg)

1. Rajendiran S, Kapoor V, Schoedel K. Fine-needle aspiration cytology of intraabdominal extralobar pulmonary sequestration: a case report. *Diagn Cytopathol* 2003; 29: 24–7.
2. Yang HJ, Lee SW, Lee HJ, et al. Extralobar pulmonary sequestration mimicking an adrenal tumor. *JSLs* 2012; 16: 671–4.
3. Kim HK, Choi YH, Ryu SM, et al. Infected infradiaphragmatic retroperitoneal extralobar pulmonary sequestration: a case report. *J Korean Med Sci* 2005; 20: 1070–2.
4. Franko J, Bell K, Pezzi CM. Intraabdominal pulmonary sequestration. *Curr Surg* 2006; 63: 35–8.
5. Gatzinsky P, Olling S. A case of carcinoma in intralobar pulmonary sequestration. *Thorac Cardiovasc Surg* 1988; 36: 290–1.
6. Schulz MD, Gill RR, Colson YL. Ipsilateral intralobar and subphrenic pulmonary sequestration. *Ann Thorac Surg* 2010; 89: 2017–9.
7. Armbruster C, Kriwanek S, Feichtinger H, et al. Intra-abdominal sequestration of the lung and elevated serum levels of CA 19-9: a diagnostic pitfall. *HPB (Oxford)* 2004; 6: 45–8.
8. Sharma S, Yadav AK, Mandal AK, et al. Enteric duplication cysts in children: a clinicopathological dilemma. *J Clin Diagn Res* 2015; 9: EC08–11.
9. Choi KK, Sung J-Y, Kim J-S, et al. Intra-abdominal bronchogenic cyst: report of five cases. *Korean J Hepatobiliary Pancreat Surg* 2012; 16: 75–9.
10. Hubli P, Rohith M, Sachin BM. A giant retroperitoneal lymphangioma: a case report. *J Clin Diagn Res* 2016; 10: PD14–5.
11. Bhandarkar DS, Smith VJ, Evans DA, et al. Benign cystic peritoneal mesothelioma. *J Clin Pathol* 1993; 46: 867–8.
12. Lee J-H, Kim M-J. Intradiaaphragmatic extralobar pulmonary sequestration in adult. *J Cardiothorac Surg* 2014; 9: 112.

DOI: <https://doi.org/10.1016/j.pathol.2019.08.008>

## Primary thyroid hyalinising clear cell carcinoma: a rare variant of salivary gland type carcinoma of the thyroid



Sir,

Clear cell carcinoma (CCC) is a rare salivary gland tumour usually arising from minor salivary glands of palate or tongue base, and it was first described by Milchgrub *et al.* in 1994.<sup>1–4</sup> CCC is characterised by small epithelioid cells with clear to eosinophilic cytoplasm and arranged in cords or nests in a hyalinised stroma. CCC usually has a disease-specific fusion of the Ewing sarcoma breakpoint region 1 (*EWSR1*) and activating transcription factor 1 (*ATF1*) gene or cAMP response element modulator (*CREM*).<sup>2,3</sup> Identification of this pathognomonic *EWSR1* rearrangement is important in the diagnosis of CCC. Herein, we report a rare case of primary thyroid CCC.

A 47-year-old woman had no previous history of systemic disease or surgery. In May 2018, a right neck mass was noted but there was no associated symptoms such as pain, tenderness, dysphagia, or odynophagia. She visited our clinic and thyroid sonography revealed a 3.5 cm right thyroid tumour. The first fine needle aspiration (FNA) reported colloid goitre. After 6 months follow-up, the thyroid tumour enlarged and the second FNA showed suspicious for malignancy. Radical thyroidectomy was performed. A white and firm tumour measuring 4.2 × 3.0 cm in size was found in the right thyroid gland (Fig. 1A). Microscopically, the tumour comprised small nests and cords of small polygonal cells with mildly irregular nuclear contours, indistinct nucleoli, and eosinophilic or clear cytoplasm (Fig. 1B,C). Most tumour nests were rimmed by a densely hyalinised stroma, while the spaces between tumour nests were less hyalinised and occasionally associated with a plasmacytic infiltrate. Two of seven level VI lymph nodes were directly invaded by the carcinoma. Immunohistochemically, the tumour cells were positive for cytokeratin (AE1/AE3) and p63 (Fig. 1D,E) but negative for TTF-1, PAX8, thyroglobulin, calcitonin, synaptophysin, chromogranin A, S100, smooth muscle actin, and SOX10. Mucicarmine stain was negative. *EWSR1* gene rearrangement in tumour cells was confirmed by fluorescent *in situ* hybridisation (FISH) using commercial Vysis *EWSR1* Dual Color Break Apart FISH Probe (Abbott Molecular, USA) (Fig. 1F). The histological and cytogenetic results confirmed a primary thyroid clear cell carcinoma. After surgery, full-body computed tomography (CT) scans showed no definite mass lesions or lymphadenopathy in the brain, head and neck, chest, abdomen, and pelvis. The patient has been followed for 6 months and there is no local recurrence or distant metastasis.

Primary thyroid salivary gland-type carcinoma is very rare, and mucoepidermoid carcinoma (MEC) and mammary analog secretory carcinoma (MASC) are the two most commonly reported salivary gland-type cancers in the thyroid gland.<sup>5,6</sup> Similar to their salivary gland counterpart, pathognomonic genetic fusions, such as *MAML2* fusion in MEC and *ETV6* fusion in MASC, can also be found in these thyroid salivary gland-type carcinomas.<sup>5–7</sup> Clear cell carcinoma is a rare, low-grade salivary gland malignancy. CCC most commonly arises from minor salivary glands of the oral